TASK 4A REPORT

PASSIVE FORCE-DEFLECTION TESTS FOR SKEWED ABUTMENTS

WITH MSE WINGWALLS

Prepared By

Kyle M. Rollins, Professor, Civil & Env. Engrg Dept., Brigham Young Univ., 368 CB, Provo, UT 84602, (801) 422-6334, rollinsk@byu.edu

Bryan Franke, Research Asst., Civil & Env. Engrg Dept., Brigham Young Univ., 368 CB, Provo, UT 84602, bryan.franke@gmail.com

Aaron K. Marsh, Research Asst., Civil & Env. Engrg Dept., Brigham Young Univ., 368 CB, Provo, UT 84602, (801) 341-9651; aaron.kirt@gmail.com

Jaycee Smith, Research Asst., Civil & Env. Engrg Dept., Brigham Young Univ., 368 CB, Provo, UT 84602, jayceeofsocal@gmail.com

Katie Palmer, Research Asst., Civil & Env. Engrg Dept., Brigham Young Univ., 368 CB, Provo, UT 84602, katienpalmer@gmail.com

Prepared for

Research Division of the Utah Department of Transportation

January 24, 2013

EXECUTIVE SUMMARY

Accounting for seismic forces and thermal expansion in bridge design requires an accurate passive force-deflection relationship for the abutment wall. Current design codes make no allowance for skew effects on passive force; however, quarter-scale lab tests indicate that there is a significant reduction in peak passive force as skew angle increases for plane-strain cases. To further explore this issue, larger-scale field tests were conducted with skew angles of 0°, 15° and 30° along with MSE wingwalls. The abutment backwall was 11-ft (3.35-m) wide by 5.5-ft (1.68-m) high and backfill material consisted of densely compacted sand. The peak passive force for the 15° and 30° skew tests was found to be 62% and 49%, respectively of the peak passive force for the 0° skew case. These results are in good agreement with the available laboratory and numerical results; however, discrepancies may suggest that backfill geometry has some effect on the reduction in peak passive force with respect to skew angle. Longitudinal displacement of the backwall at the peak passive force was found to be approximately 5% of the backwall height for the 0° skew test and 3% of the backwall height for the 15° and 30° skew tests. Larger deflection (5% of the backwall height for the 0° skew test) is consistent with previously reported values for large-scale passive force-deflection tests with MSE wingwalls; however, the lower deflection at failure for the skew tests was not expected. Passive pressure across the backwall was initially uniform but became non-uniform at larger displacements with the highest values near the backwall edges and the peak pressure at the acute corner. Shear force on the backwall increased as skew angle increased despite the reduction in longitudinal force with skew angle. Transverse pile-cap displacement also increased with skew angle and was sufficient to mobilize the frictional resistance. Vertical heave for the 0°, 15° and 30° tests were quite typically 3% of the fill height; however, maximum outward wingwall displacement increased for the obtuse wingwall with increasing skew angle. The maximum outward displacement of the wingwall on the acute side remained relatively unchanged for any skew angle.

INTRODUCTION

Various researchers have conducted large-scale field studies to investigate passive force-deflection behavior with densely compacted granular backfills (Cole and Rollins 2006; Duncan and Mokwa 2001; Lemnitzer et al. 2009; Rollins and Sparks 2002). The results of numerous field studies show that the ultimate passive force may be adequately predicted using the log-spiral method and develops at displacements of approximately 3% to 4% of the wall height (Cole and Rollins 2006; Lemnitzer et al. 2009). Additionally, since soil embankments adjacent to bridge structures commonly utilize MSE (mechanically stabilized earth) systems, some of these studies have also been designed to address configurations including MSE wingwalls (Rollins et al. 2010). Two general models (bilinear and hyperbolic) have been suggested to approximate the passive force-deflection curves. The best approximation is achieved using various hyperbolic models (Duncan and Mokwa 2001; Shamsabadi et al. 2006; Shamsabadi et al. 2007); however, for simplicity, most design methods implement bilinear methods (AASHTO 2011; Caltrans 2010).

Specific differences have been identified between results obtained from the unconfined backfill tests and results obtained from tests with MSE wingwalls. First, the ultimate passive force per width achieved for tests with MSE wingwalls was higher than that predicted using the log-spiral method with the triaxial friction angle. Consequently, in order to estimate more accurately the ultimate passive force with MSE wingwalls, the plane-strain friction angle, ϕ_{ps}, must be used instead of the triaxial friction angle, ϕ. Therefore, for general application, the plane-strain friction angle should be approximately 10% to 12% higher than the triaxial friction angle (Kulhawy and Mayne, 1990)(Rollins et al., 2010). Secondly, as a result of outward, transverse movement of the MSE wingwalls, larger longitudinal movement—typically 4% to 5% of the wall height—was necessary to mobilize the ultimate or peak passive force.

In the past, the ultimate passive resistance has been calculated in the same manner for both skewed and non-skewed bridge abutment geometries. Furthermore, passive force-deflection relationships have been treated in a similar fashion. Some case studies, however, have shown substandard performance

for bridges with skewed abutments versus those with non-skewed abutments. Such evidence has been noted in numerous reports and publications as a result of thermally induced stresses and following severe seismic events (Apirakvorapinit et al. 2012; Elnashai et al. 2010; Unjoh 2012). In recent years, two separate studies have investigated the effects of skewed bridge geometry on ultimate passive force and passive-force deflection behavior. Shamsabadi et al., 2006, employed three-dimensional, nonlinear, finite-element models to explore the differences between passive soil capacities for skewed and non-skewed bridge abutments. The results of these numerical models suggest a significant reduction in passive soil resistance for skewed bridge abutment geometries. These findings were subsequently confirmed by small-scale lab tests with a 0.61-m (2.0-ft) high wall (Rollins and Jessee, 2012). Using data from these two studies, Rollins and Jessee, 2012, proposed the reduction factor, R_{skew}, given in Equation 1 as a function of skew angle, θ (degrees). This proposed relationship effectively reduces the non-skewed passive force, P_p, for skewed bridge abutments. Using Equation 2, this reduction factor can be used to obtain the reduced passive force, P_{p-skew}, for skewed bridge abutments.

$$R_{skew} = 8.0 * 10^{-5}\theta^2 - 0.018\theta + 1.0 \qquad (1)$$

$$P_{p-skew} = P_p R_{skew} \qquad (2)$$

Recently, large-scale, passive force-deflection tests were completed to assess these researchers' findings. Additionally, these tests explored the effect of various abutment geometries and backfill properties. In this study, three large-scale tests were performed with skew angles of 0°, 15, and 30° using an existing pile cap, which was 15-ft (4.6-m) long, 11-ft (3.4-m) wide and 5.5-ft (1.7-m) high and has been used in several past field studies (Rollins and Sparks 2002; Rollins et al. 2010; Strassburg 2010). Concrete wedges were attached to the face of the pile cap to create the skewed geometry necessary for testing. Only a brief background, a description of test layout and procedures, a brief report of applicable results, and a general comparison of these three large-scale tests are provided in this document.

BACKGROUND

As a bridge deflects into the soil at the abutment, different interaction forces are present between the bridge structure and the abutment for a bridge with skewed geometry (see

Figure 1). At this interface, the longitudinal force, P_L, acts parallel to the bridge structure. This driving force may be broken into two components: a component acting normal, $P_L\cos\theta$, (see Equation 3) and a component acting parallel, P_T, (see Equation 4) to the abutment backwall face. To ensure stability, of the bridge structure, the passive soil resistance, P_p, and shear resistance, P_R, (see Equation 5) provided by the soil backfill and bridge abutment must resist this driving force. Therefore, force and moment equilibrium must be maintained (see Equation 6 and 7). In these equations, θ is the backwall skew angle, c is soil cohesion, A is backwall area, δ is the abutment backwall-soil interface friction angle, F_s is the factor of safety, and L is the length of the bridge. If the soil cohesion is neglected (assumed to be 0), bridge stability becomes independent of passive force. In this case, if a typical design backwall-soil interface friction angle of 22° is assumed for a bridge abutment with a skew angle of 15°, the factor of safety easily decreases below 1.5 (Burke, 1994). Additionally, the validity of these equations hinges on the stability of the bridge. In the cases of bridge rotation or excessive longitudinal movement, these relationships do not apply.
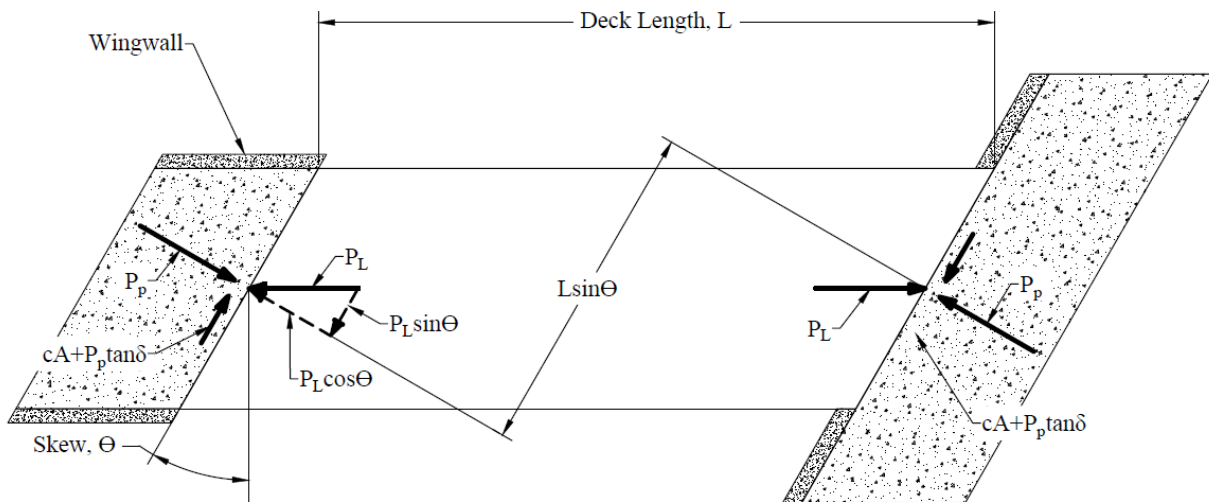
Figure 1. Conceptualized Interaction Forces Between Bridge Structure and Skewed Abutment

$$P_p = \dot{P}_L \cos \theta \tag{3}$$

$$P_T = P_L \sin \theta \tag{4}$$

$$P_R = cA + P_p \tan \delta \tag{5}$$

$$\frac{cA + P_p \tan \delta}{F_s} \geq P_L \sin \theta \tag{6}$$

$$\frac{cA + P_p \tan \delta \;\; L \cos \theta}{F_s} \geq P_p L \sin \theta \tag{7}$$

TEST CONFIGURATION

The test setup for the lab tests (See Figure 2) involved a 2-ft (0.61-m) high by 4-ft (1.22-m) wide backwall with a 2D or plane-strain backfill geometry (Rollins and Jessee 2012). In contrast, this study was completed using an existing pile-cap; therefore, details regarding the specific site may be found in other publications (Christensen 2006; Rollins et al. 2010; Strassburg 2010). Additionally, test-specific site characterization is provided in this section.
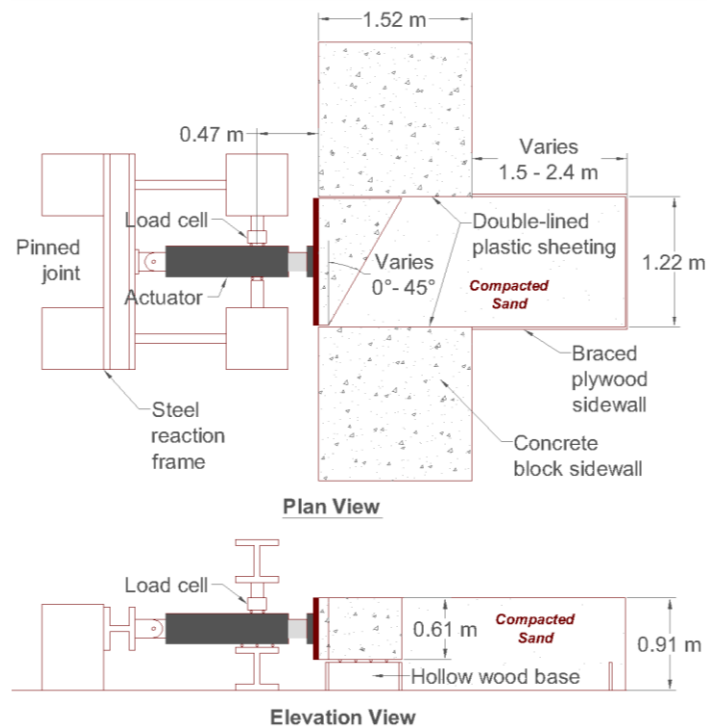
Figure 2. Schematic Drawings of Lab Test Layout (Rollins and Jessee 2012) (Note: 1 m = 3.28 ft).

Test Layout

The backfill zone was approximately 11-ft (3.4-m) wide and extended 24 ft (7.3 m) longitudinally from the backwall (pile-cap) face for the 0° skew test; however, since an additional concrete wedge was affixed to the existing pile cap (see Figure 3), the backfill extended approximately 24 ft (7.3 m) longitudinally from the acute corner of the skew. Additionally, since the native soil was significantly stronger than the backfill material, the bottom of the test pit adjacent to the backwall was placed approximately 1.0 ft (0.30 m) below the bottom of the pile-cap and extended 10 ft (3.1 m) longitudinally from the backwall face for both tests. Beyond this region, however, the test pit tapered becoming level with the bottom of the pile cap. This prevented any interference from the native soil in the development of the suspected, log-spiral failure surface and reduced the required volume of backfill material.

To effectively attach the concrete wedge to the pile-cap face for 15 and 30° skew tests, concrete wedges were placed atop a set of rollers resting on small platform beneath the concrete wedge. This minimized friction between the concrete wedge and underlying soil. In addition, it ensured that lateral resistance was due only to the passive soil resistance provided by the backfill material and the piles beneath the existing pile cap. Preliminary testing with no backfill, showed a negligible increase in lateral resistance as a result of the additional concrete wedge.

These large-scale tests were similar to the Rollins and Jessee, 2012, plane-strain lab tests; similarly, the backfill was confined with MSE wingwalls; however, the use of MSE wingwalls also introduced steel reinforcements into the backfill soil. Each side consisted of two 12-ft (3.7-m) long by 5.5-ft (1.5-m) high by 6.0-in (15-cm) wide, concrete MSE panels restrained with four steel reinforcing bar mats per panel. The upper grids were approximately 68-in (1.7-m) long by 32-in (0.81-m) wide and the lower grids were approximately 68-in (1.7-m) long by 40-in (1.0-m) wide. Also, the design pullout resistance determined using guidelines specified by the FHWA (Federal Highway Administration) was approximately 2.3 kip (10.2 kN) and 9.6 kip (42.6 kN) for the upper and lower reinforcement grids, respectively (Elias and Christopher 1997).
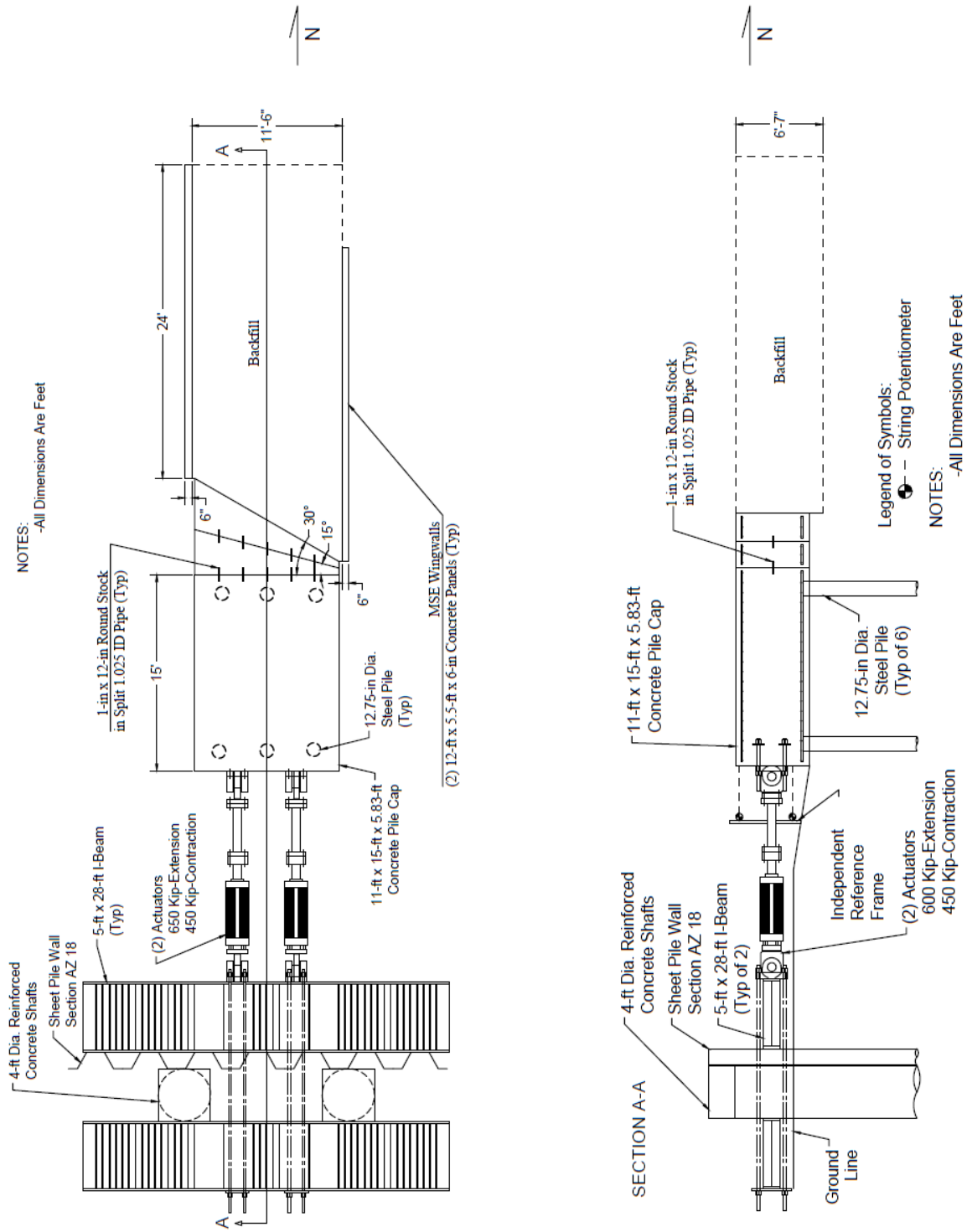
Figure 3. 30° Skew Test Configuration with Concrete Wedge and MSE Wingwalls.

Backfill Characterization

Backfill soil used for this series of tests consisted of approximately 250 tons (227 metric tons) of poorly graded sand (SP type soil according to the Unified Soil Classification System or an A-1-b type soil according to the AASHTO Classification System). Gradations before and after the test series found that the coefficient of uniformity (C_u) and coefficient of curvature (C_c) were 7.6 and 0.8 pre-test, and 9.7 and 0.7 post-test, respectively. This variability is likely due to small differences in soil samples. For comparison, the C_u and C_c values from the lab tests were 3.7 and 0.7, respectively.

Figure 4 also shows the soil gradation for the lab tests.

Unit Weight and Moisture Content

The maximum dry density and optimum moisture content were determined to be 111.5 pcf (17.5 kN/m^3) and 7.1%, respectively, in accordance with the modified Proctor compaction test (ASTM D1557). Compaction, however, was found to be much easier in the field when the moisture content was approximately 9%. Onsite, the target compaction level was 95% of the modified proctor maximum. This was accomplished using a vibratory smooth drum roller compactor and vibratory plate compactor to successively compact 6-in (15 cm) lifts of backfill material. Throughout testing, a calibrated nuclear density gauge was used to ensure proper compaction and moisture content. Though not shown, the variation of relative compaction and moisture content with depth was not significant. Relative density was estimated using the empirical relationship between relative density (D_r) and relative compaction (R) for granular materials developed by Lee and Singh (1971) as shown in Equation (8).

$$R = 80 + 0.2D_r \qquad (8)$$

A summary of soil compaction, density and water content is provided in Table I. The properties of the three backfills were generally very consistent. Average relative compaction, relative density, and water content for the three tests were 96.9%, 84% and 9.1%, respectively. For comparison purposes the average relative compaction, relative density, and water content for the laboratory tests were 97.9%, 90%, and 8.0%, respectively (Rollins and Jessee 2012).
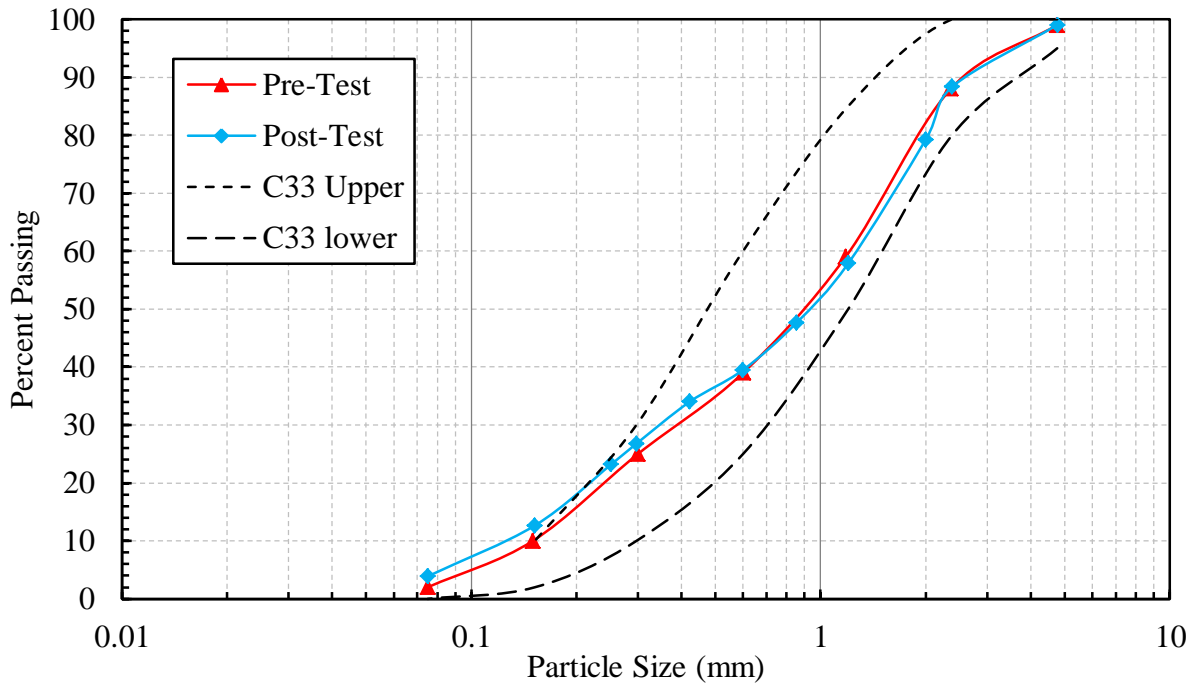
Figure 4. Gradation for Backfill Sand Relative to Concrete Sand Gradation (Note: 1 in = 25.4 mm).

TABLE I. COMPACTION, DENSITY AND MOISTURE CONTENT SUMMARY

	0° Skew Test	15° Skew Test	30° Skew Test
Minimum Dry Unit Weight (pcf) [kN/m³]	110.0 [17.3]	110.8 [17.4]	110.3 [17.3]
Maximum Dry Unit Weight (pcf) [kN/m³]	104.8 [16.5]	106.4 [16.7]	105.2 [16.5]
Average Dry Unit Weight (pcf) [kN/m³]	107.5 [16.9]	108.4 [17.0]	108.0 [17.0]
Relative Compaction (%)	96.4	97.3	96.9
Relative Density (%)	82	87	84
Moisture Content (%)	9.1	8.9	9.2

Shear Strength

Direct shear tests were conducted at the field density and moisture content values. The drained friction angle, ϕ', was found to be 41° and cohesion, c, was found to be approximately 100 psf (4.79 kPa). Previous researchers (Cole and Rollins 2006; Rollins and Jessee 2012) conducted direct shear tests and determined that the interface friction angle, δ, between similar sand and concrete was about 75% of the soil friction angle ($\delta/\phi = 0.75$). For purposes of comparison, the drained friction angle of the sand

used for the laboratory skew tests was 46° with and the cohesion was 70 psf (3.35 kPa) (Rollins and Jessee 2012).

Instrumentation

Hydraulic actuators, fitted with pressure transducers, were used to apply and measure longitudinal forces during testing. Although the longitudinal extension/contraction of the actuators was also measured, to eliminate potential lateral displacement of the reaction frame, four string potentiometers (string pots) attached to the back side of the pile cap were used to measure pile-cap displacement relative to an independent reference frame. Longitudinal displacement of the pile cap was confirmed using independent measurements from inclinometer and shape array readings taken at both the north and south ends of the pile cap.

Before testing, a grid of 2.0-ft (0.61-m) squares—refined to a grid of 1.0-ft (0.30-m) squares near the backwall—was painted on the surface of the backfill. The relative elevation change at grid-intersection points was measured using a surveying level and rod before and after each test to determine vertical heave. This grid also helped to identify surface cracks and relative horizontal displacement for the 15° test.

Additionally, pressure was measured normal to the backwall face using pressure plates located approximately 22 in (0.56 m) up from the base of the wedge and 21.5 in (0.546 m) center to center across the width of the wedge for the 30° test alone. Because some researchers have suggested a more triangular pressure distribution along the backwall face for skewed geometries (Sandford and Elgaaly, 1993; Shamsabadi et al., 2006), this was done to understand the pressure distribution along the backwall face for skewed abutments with MSE wingwalls.for the 30° test alone.

Testing Procedure

Before the MSE wingwalls and backfill material were placed, lateral load tests of the piles and cap (no backfill and no MSE wingwalls) were performed to provide a baseline or correction curve for

subsequent testing with backfill material. Because the pile cap had been previously employed for a number of tests, the baseline resistance has become relatively linear.

After the placement of backfill material with MSE wingwalls and reinforcing grids in place, instrumentation was checked and initialized to begin testing. The pile cap was displaced longitudinally into the backfill material at a constant rate of displacement [0.25 in/min (6.35 mm/min)]. At displacement intervals of approximately 0.25 in (0.64 cm), the pile-cap position was held constant for approximately 2 minutes while cracks on the surface of the backfill material were identified and other visual observations were recorded; however, continuous data were collected from all instrumentation during testing. For analysis, data points associated with each 0.25-in (0.64-cm) displacement were identified. At completion, the maximum longitudinal, pile-cap displacement for the 0°, 15° and 30° skew tests was 3.18 in (8.08 cm), 3.23 in (8.20 cm) and 3.48 in (8.84 cm), respectively.

TEST RESULTS

Discussion in this section covers passive force-deflection behavior, backfill crack patterns, and vertical deflection of backfill material for the 0°, 15° and 30° skew tests. Also, results from this study and the applicable results obtained from previously completed testing (Rollins and Jessee 2012; Shamsabadi et al. 2006) are provided in this section.

Passive Force-Deflection

The longitudinal force measured by the actuators was reduced by the lateral resistance provided by the piles and cap using the "baseline" curves for both tests. For the 15° and 30° skew test, the passive force was equal to the component of longitudinal force normal to the backwall face as given by Equation 3. The passive-force deflection curves for the 0°, 15° and 30° skew tests are shown in Figure 5. For the 0° skew test, the longitudinal force became so large in the process of testing that the capacity of the actuators became a challenge. Consequently, the curve did not appear to plateau; therefore, the maximum load was associated with the last displacement (slightly over 5% of wall height). Despite the fact that the 0° skew

curve does not appear to have reached ultimate point of failure, this study still shows a significant reduction in passive force as a result of the skew.

Not only was there a significant reduction in ultimate passive force, but the failure also seemed to develop somewhat sooner with the 15° and 30° skew angles. The maximum passive force was obtained with a pile-cap deflection of approximately 5% of the wall height for both tests; however, the 15° and 30° skew tests experienced a substantial decrease in the rate of strength gain at a displacement of approximately 3% of the wall height. This relatively flat plateau in the load-displacement curve was also observed in the lab tests involving skews. Despite this observation, the soil stiffness appears to have remained largely unaffected for small displacements.

Figure 6 compares normalized passive force-displacement curves for the field tests conducted in this study and the lab tests conducted by Rollins and Jessee (2012). In this plot, passive force is normalized to the projected backwall area [e.g. 5.5 ft (1.68 m) by 11 ft (3.35 m) rather than 5.5 ft (1.68 m) by 12.7 ft (3.87 m)]. Also, displacement is normalized to backwall height to facilitate the comparison between the field and lab tests.

As the lab tests were conducted so as to simulate plane-strain conditions, and the field tests used plane-strain conditions with MSE wingwall confinement, the higher normalized passive force for the lab tests is not surprising because the soil for the lab tests was compacted to a higher relative density. In addition to the higher normalized peak passive force for the 0°, 15° and 30° skew lab tests, the lab tests developed the peak passive force at deflections between 2% and 3% of the backwall height. However, the peak passive force for the field tests developed at longitudinal deflections between 2% and 3% of the backwall height, H, for just the 15° and 30° skew tests and approximately 5% to 6% of the backwall height for the 0° skew test. The greater drop in passive force after the peak for the lab tests is consistent with the fact that the lab tests were compacted to a denser state and would therefore have had a greater tendency to dilate and experience a decrease in strength during shearing. The denser state may explain the somewhat more brittle behavior for the lab tests as well.

The results of this study also correlate very well with the results obtained previously (see Figure 7). The reduction curve proposed by Rollins and Jessee (2012) predicts a reduction factor, R_{skew}, of 0.75 and 0.53 for the 15° and 30° skew tests, respectively. The back calculated R_{skew} values for this field study are 0.62 and 0.49 for the 15° and 30° skew tests, respectively. These are both a little lower than the values predicted by the curve proposed by Rollins and Jessee (2012). This may be a consequence of the reduced side restraint provided by the MSE walls versus the concrete block sidewall used in the lab tests. Further testing should be performed to confirm this observation.
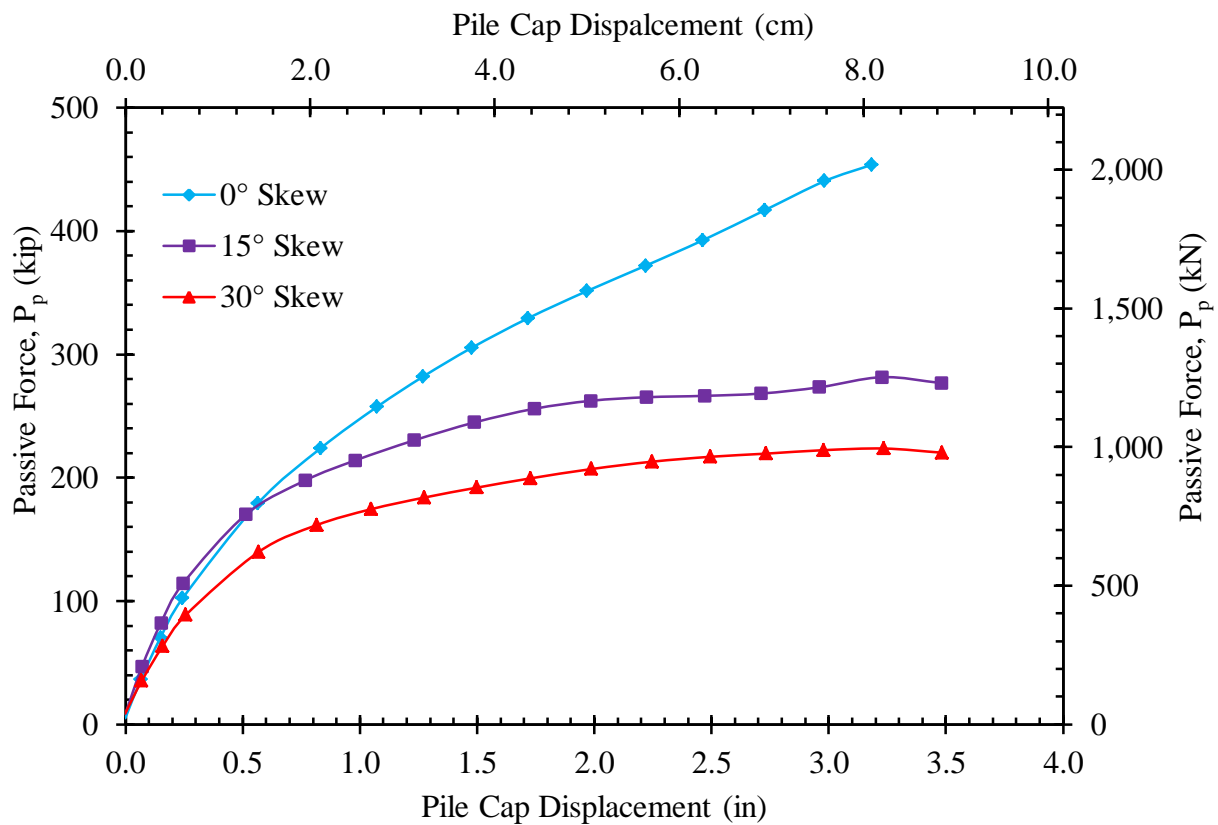
Figure 5. Passive Force-Deflection Curve for 0°, 15° and 30° Skew Tests with Densely Compacted Granular Backfill.
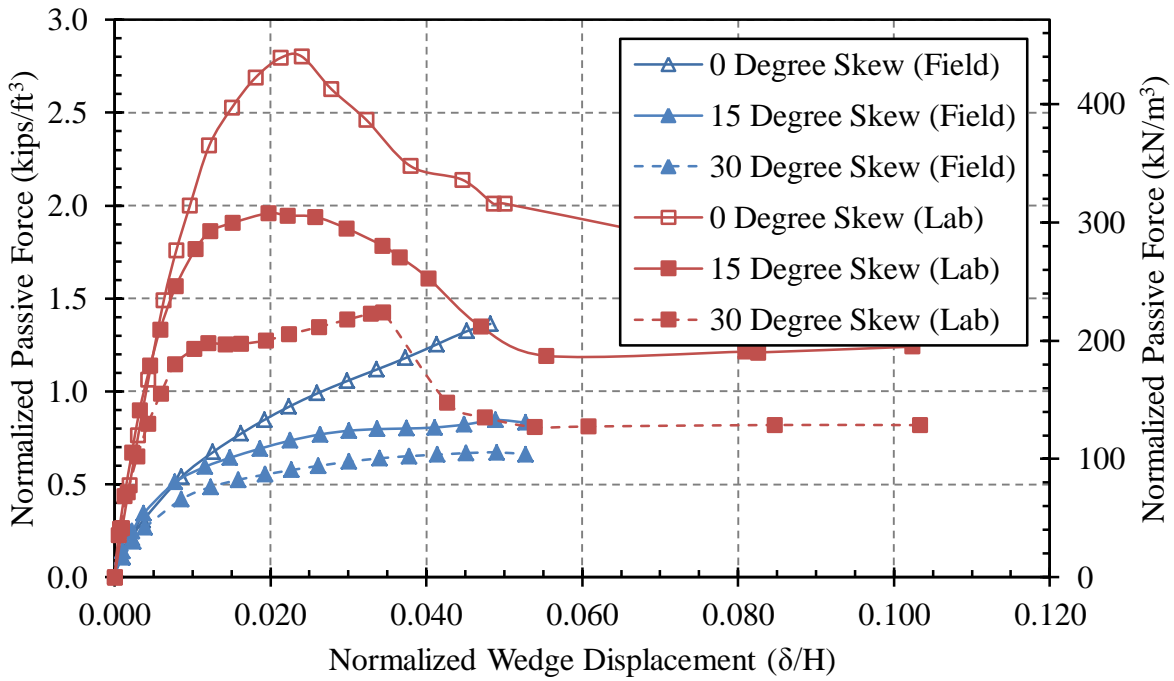
Figure 6. Passive Force-Deflection Curves for Field and Lab Tests with Passive Force Normalized to the Projected Width of the Backwall Multiplied by the Backwall Height Squared Versus Backwall Deflection Normalized to Backwall Height.

$$R_{skew} = 8E\text{-}05\theta^2 - 0.018\theta + 1.0$$
$$R^2 = 0.98$$
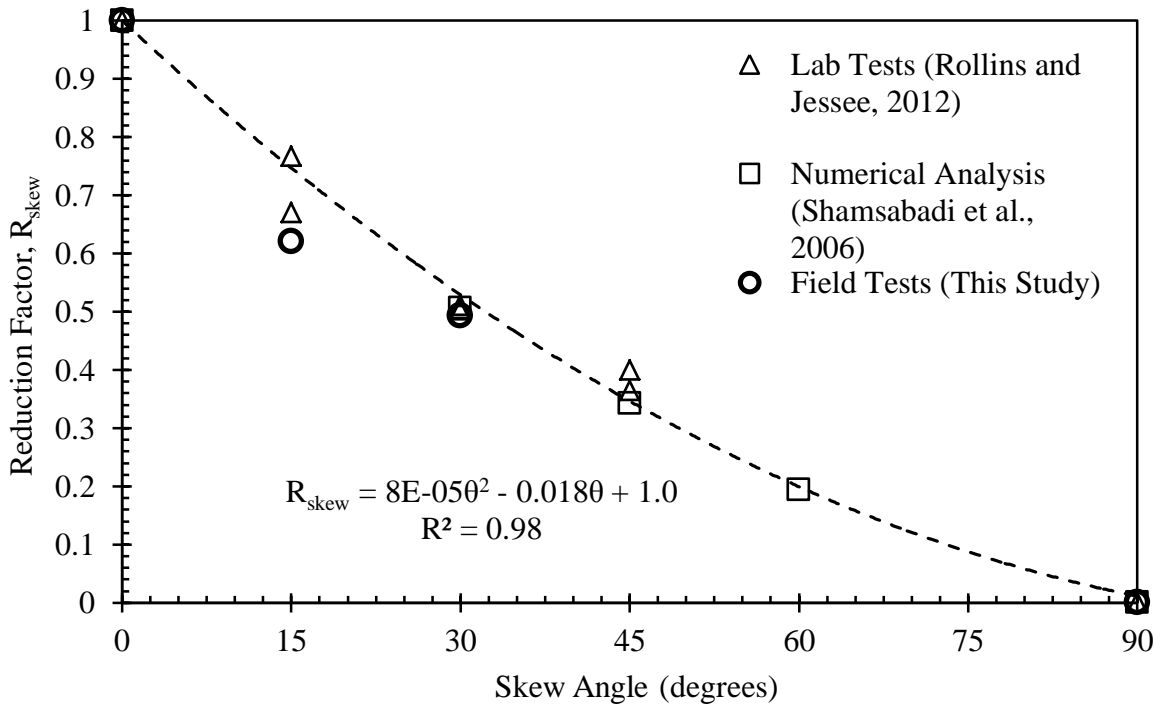
Figure 7. Reduction Factor, R_{skew}, Plotted Versus Skew Angle with Proposed Reduction Curve.

Pile-Cap Displacement vs. Depth

Figure 8 provides longitudinal deflection versus depth profiles obtained from both an inclinometer and a shape accelerometer array for the 15° skew test. Both profiles represent pile-cap behavior for the final longitudinal displacement of the test. The depths are referenced to the top of the cap. The average deflections measured by two sets of string pots (each set at a different elevation on the pile cap) are also shown in Figure 8 for comparison purposes. The graph demonstrates that the measurements obtained by the three systems were reasonably accurate and comparable to each other. The percent difference between the inclinometer and shape array profiles from the top of the cap to a depth of 20 ft (6 m) ranges between 0.55 and 12.8% with an average of 5.3%. The displacements below a depth of 20 ft (6 m) are very small and the error values in this zone are not particularly meaningful. Similarly, good agreement was obtained between the shape array and inclinometer for the other tests. Also, the percent difference between the displacements measured by the inclinometer and the string pots is 1.4 and 1.8% for the upper and lower string pots on the back of the pile cap, respectively, with an average of 1.6%.

The measurements indicate a relatively liner deflection profile within the pile cap with small pile-cap rotations. Below the base of the cap, the piles deflect in a non-linear fashion with the deflections reaching a point of counter flexure at a depth of approximately 21 ft (6.3 m) and a point of fixity at about 31 ft (9.5 m). Agreement between the north and south inclinometers was generally very good.

Transverse deflection versus depth profiles for the pile cap, recorded by shape array, inclinometer, and LVDTs, are also plotted in Figure 9. Plotted on a smaller scale, the percent error seems larger than the longitudinal error although the magnitude difference is small. However, as observed for the deflections below 20 ft (6 m) in the longitudinal test, the percent difference is exaggerated due to the smaller scale. The percent difference is generally within the error thresholds of each instrument (±1.5 mm/30 m for shape array, and ±1.24 mm/30m for inclinometer (Rollins et al, 2009). Error relative to the transverse LVDTs is due to the lower LVDT being only relatively fixed, and therefore moving with the soil near the pile cap. This resulted in inaccurate lateral deflection at the bottom of the pile cap. Results

are similar for the tests at other skew angles. Once again, the shape of the deflection profile indicates essentially linear deflection in the pile cap and very small rotations. The deflection in the piles is non-linear and decreases toward zero at a deflection of about 25 ft (7.6 m).

Although the inclinometer readings were only taken at the maximum deflection for each load test, shape array profiles in the longitudinal and transverse directions were obtained at each deflection increment for each test. For example, Figure 10 shows profiles of longitudinal deflection vs. depth for each deflection increment. As the deflection level increases the deflection of the pile cap remains linear but the rotation progressively increases while the depth to the point of fixity increases. Similar curves were obtained in the transverse direction. At smaller deflection levels there are some variations associated with the small measurement errors; however at larger deflections, the data was accurate and useful in visualizing the pile movement.
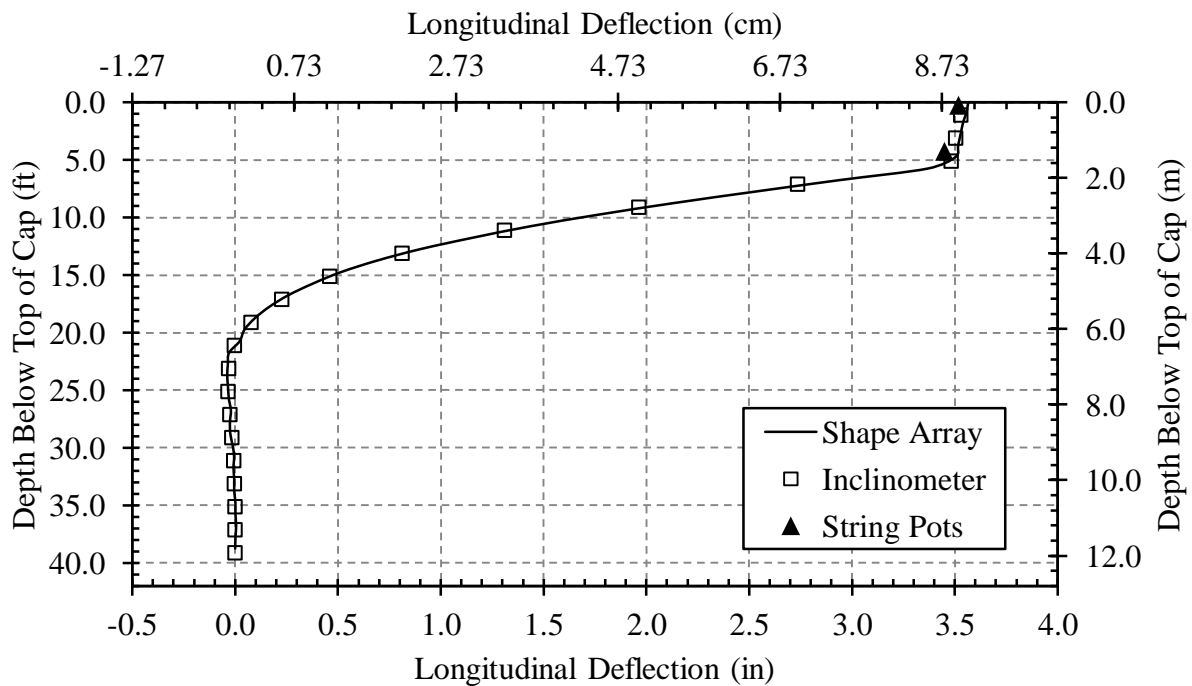
Figure 8. Final Longitudinal Deflection for 15° Skew Test Comparing North Inclinometer and Shape Array with String Potentiometers.
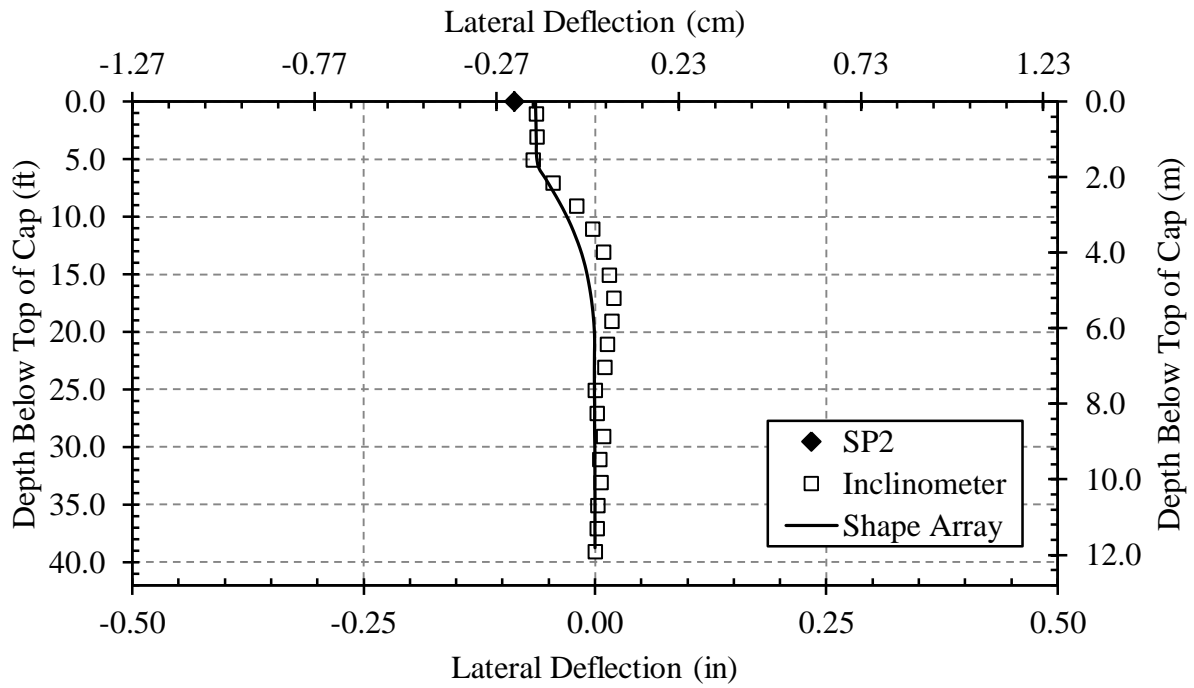
Figure 9. Final Transverse Deflection for 15° Skew Test Comparing North Inclinometer and Shape Array with String Potentiometers and LVDTs.
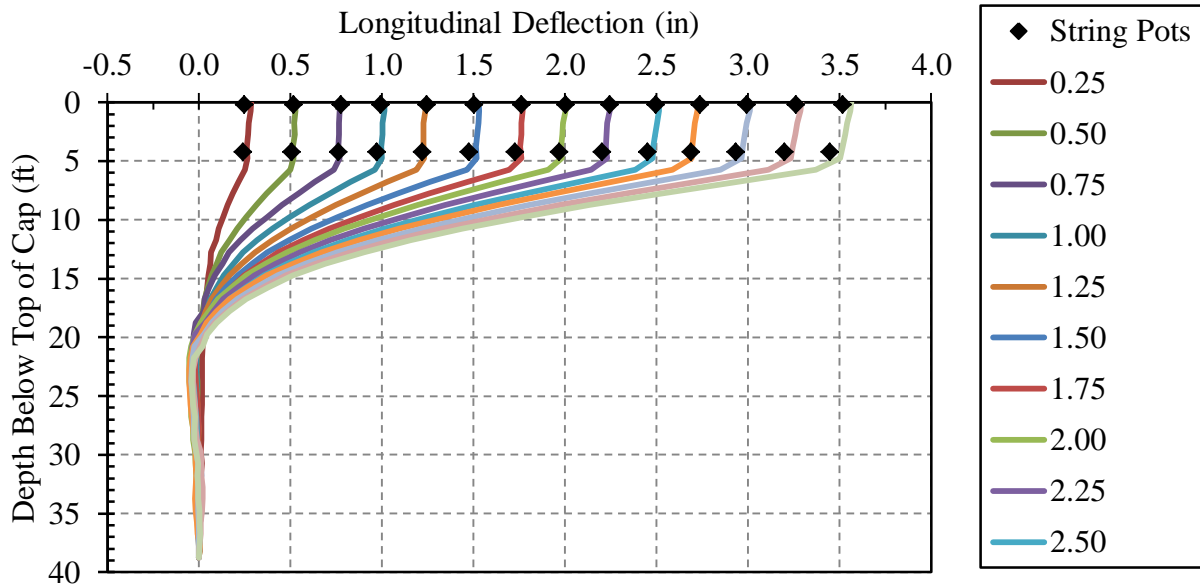
Figure 10. Longitudinal Deflection vs. Depth From SAA Data at Various Deflection Increments for 15° Skew Test.

As noted previously, the inclinometer and shape arrays measured transverse deflections for the north and south ends of the pile cap with respect to depth. The measured transverse deflections at the top of pile cap on for both the north and south ends of the pile cap after the last deflection increment are plotted in Figure 11 in a plan view perspective for each test. By connecting these points on the north and south sides, the rotation of the cap can be visualized. Although deflections of both actuators were kept relatively constant throughout the test, rotation and transverse deflection were still affected by the skew angle. As seen in Figure 11, counter-clockwise rotation of the pile cap was observed for all of the tests. The average transverse deflection for 0° and 15° skew tests were 0.052 in (1.3 mm); however, for the 30° skew, the pile cap experienced larger transverse deflection [0.15 in (3.8 mm)] in the direction of the skew. Rotation remained relatively small for all tests ranging in magnitude from 0.12 to 0.42 degrees.
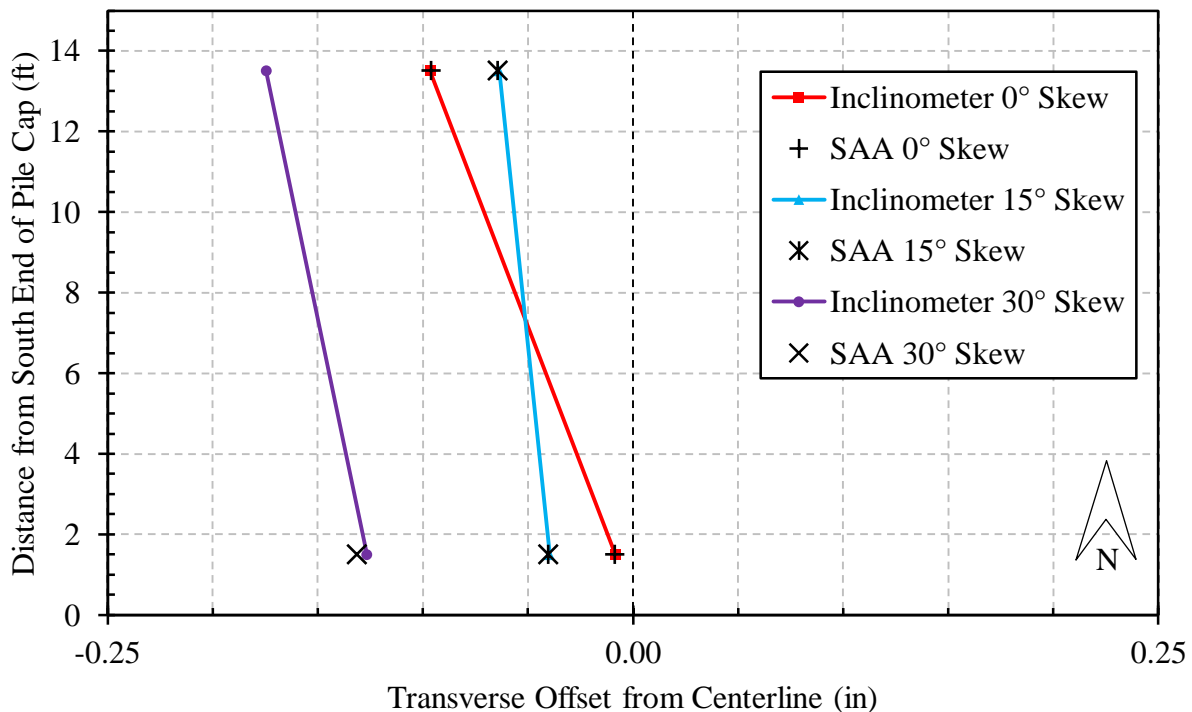
Figure 11. Transverse Pile-Cap Deflection and Rotation Determined Between North and South Shape Array and Inclinometer Data.

Backwall Pressure

Figure 12 shows the measured pressure distribution across the width of the pile cap for a series of pile-cap displacement increments. Analysis of results reveals that the pressure was relatively uniform across the wall face for the first inch of displacement (Figure 12-A & Figure 12-B). At higher displacements, the pressure then increased somewhat along the outside edges of the pile cap (Figure 12-C). As the passive force reached a maximum and the soil sheared, the pressure distribution became more parabolic in nature (Figure 12-D. The maximum values were measured on the acute corner of the pile cap at a displacement of approximately 3.5 inches. As the cap continued to move forward, the new pressure distribution slowly increased near the edges, finishing with the highest pressure on the acute corner. The lowest pressure was located in the center of the pile cap wall (Figure 12-E); in fact, the pressures actually began to decrease in the middle with increasing pile-cap movement. The complete pressure distribution progression can be seen in Figure 12-F.

Results from this test do not seem to agree completely with findings obtained by Sandford and Elgaaly (1993) in which, the pressure on the obtuse side of a fully functioning bridge abutment was significantly greater than on the acute side (see Figure 13). Marginally higher pressures were observed on the west edge of the backwall (acute corner of the skew) compared to pressure measured on the east (obtuse corner). The higher pressures may indicate additional frictional resistance provided by the soil-wingwall interface, as well as increased vertical restraint (as a result of the steel reinforcing grids) perpetuating backfill shear failure. Additionally, the pressure distribution results from these large-scale tests vary from Sanford's on the acute side of the pile cap where pressures were predicted to be the smallest but were largest and actually much greater than in the middle of the pile cap. It should be noted; however, that Stanford only measured pressure at two points, thus the complete pressure distribution is not accurately known.
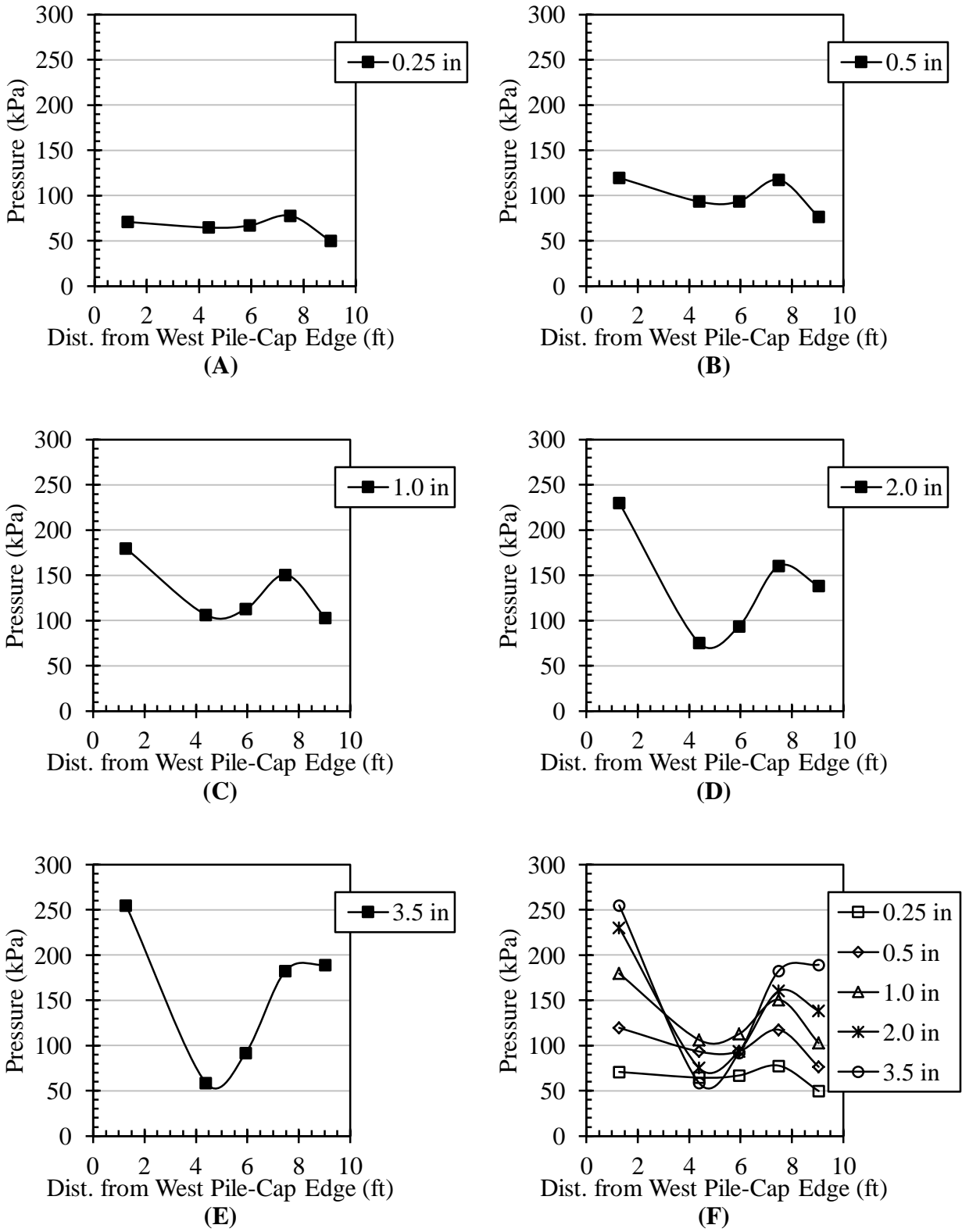
Figure 12. Progression of Horizontal Pressure Distribution with Longitudinal Pile-Cap Displacement.
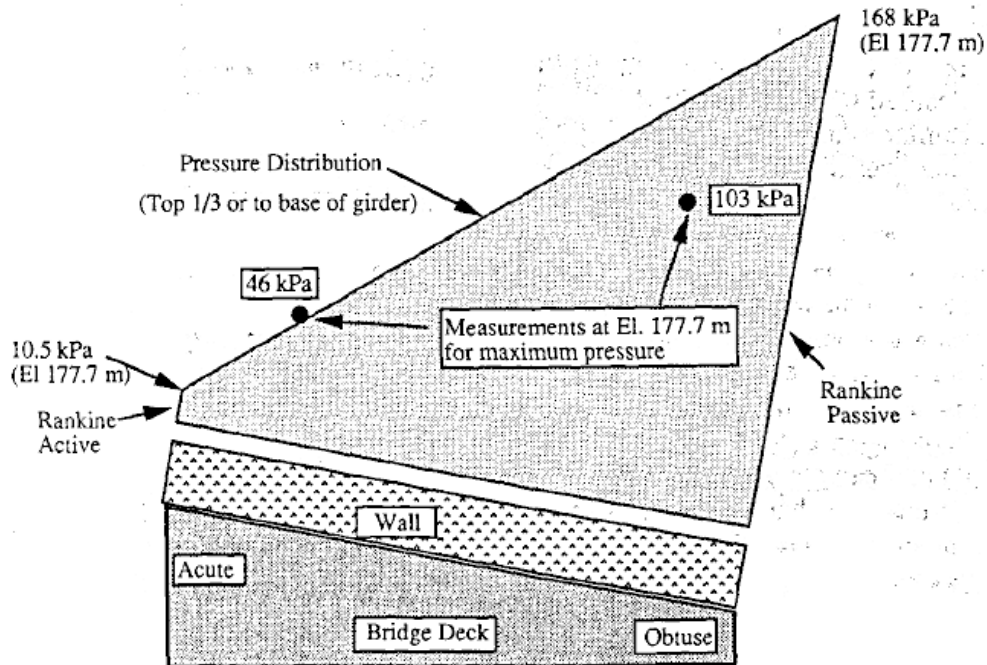
Figure 13. Design Lateral Pressure Distribution for Skewed Abutments (Sandford and Elgaaly 1993).

Although findings from displacement instrumentation reveal that the pile cap rotated slightly counterclockwise and displaced to the left, rotation of the pile cap was greatly restricted by the actuators and underlying piles. By significantly reducing this parameter, it can be implied that rotation is not the only cause of a variance in pressure distribution. Results from this study reveal that higher pressures can still develop on the outside edges of the cap even if the pile cap is restrained and rotation is relatively small.

Applied Shear Force vs. Transverse Displacement

Equipment malfunctions resulted in the loss of transverse deflection data for the 30° skew test. As a result, only the relationship between applied shear force, P_T, and transverse displacement for the 15° skew test is shown in Figure 14. The applied shear force was computed using Equation (4) and displacement values were based on shape array measurements taken during testing. In Figure 15, the shear force has been normalized by the maximum shear force.
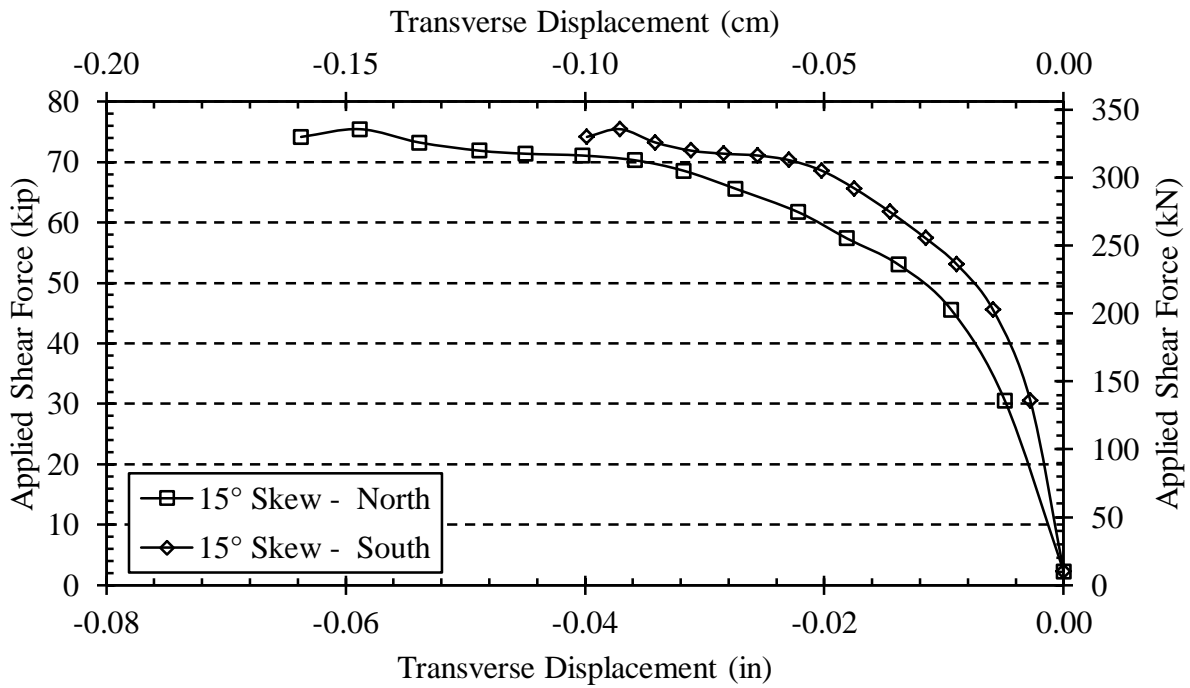
Figure 14. Applied Shear Force Versus Transverse Displacement.
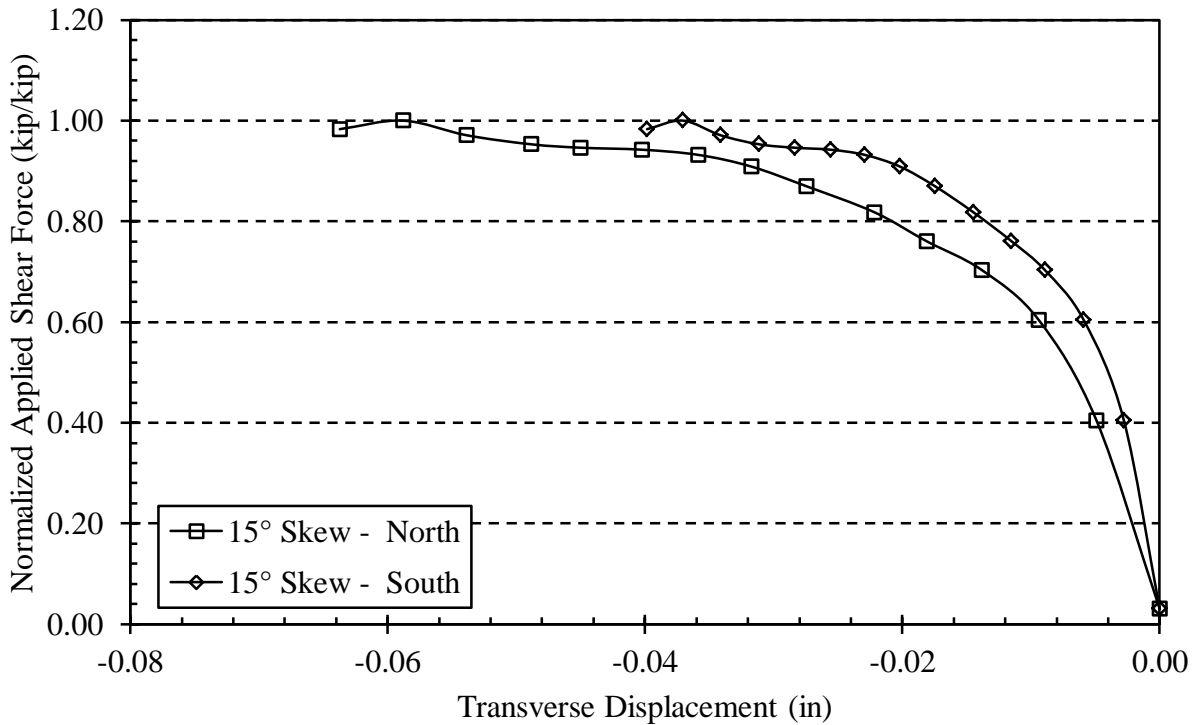
Figure 15. Normalized Applied Shear Force Versus Transverse Displacement.

According to Duncan and Mokwa (2001), the amount of movement required to mobilize skin friction on an interface is typically between 0.10 and 0.25 inch. The measured displacement is lower than these limits, therefore, the applied shear force could be less than the shear resistance, P_R, provided by the abutment wall. In a subsequent report, the shear resistance will be calculated once the interface friction angle and cohesion on the pile cap have been more accurately assessed.

Failure Surface Geometry

Backfill displacement was located primarily in the region associated with a typical log-spiral failure surface; however, general movement of the entire backfill region was observed. This effect became less pronounced for the 30° skew test. Vertical displacement was recorded at each surface grid intersection point before and after each test. Using these data points, contour maps of the backfill region were created. Plots of the heave contours at the completion of the 0°, 15° and 30° skew tests are shown in Figure 16, Figure 17, and Figure 18, respectively. Cracking patterns are also shown. Contouring was generated using Microsoft Excel with VBA (Visual Basic) to generate 3D scatter points and Linear or IDW (Inverse Distance Weighted) interpolation techniques provided in GMS 9.0 (Groundwater Modeling System) distributed by Aquaveo, LLC. As a result of the skewed geometry present in the 30°-skew contour map, the rapid decrease in vertical displacement near the backwall may simply be an artifact attributed to use of a square contouring region not aligned with the skewed interface.

Generally, the maximum vertical heave was located between 2 ft and 10 ft (0.61m and 3.05 m) longitudinally from the backwall face. The maximum vertical displacement was 1.80 in (45.7 mm), 1.92 in (48.8 mm), and 2.04 in (51.8 mm) for the 0°, 15° and 30° skew tests, respectively. However, because the level rod used to measure vertical displacement was to the nearest 0.01 ft or 0.12 in (3 mm), these vertical displacements are likely within the expected margin of error. Therefore, it is reasonable to assume that the magnitude of vertical displacement remained roughly the same for the three tests. Consequently, the maximum vertical heave was approximately 3% of the backwall height. Additionally, for the 15° and 30° skew test, the zone of maximum backfill heave shifted to the acute side of the skew. Additionally, the

heave observed on the obtuse side of the skew decreased with increasing skew angle. This observation is consistent with the larger pressure measured on the backwall face.
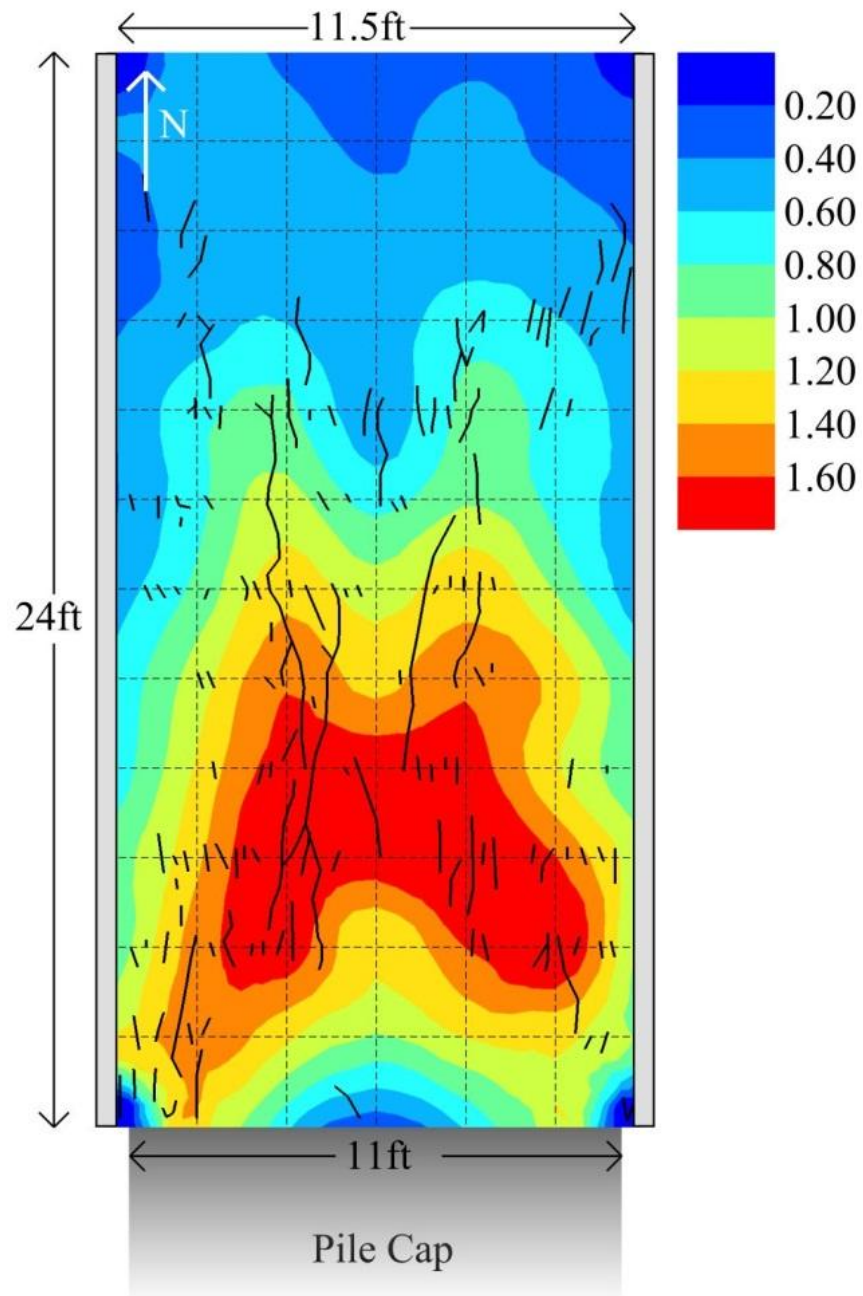
Figure 16. Vertical Backfill Displacement (Heave) in Inches for 0° Skew Test [Note: 1 in. = 25.4 mm and Gridlines are Spaced at 2-ft (0.61-m) Intervals].
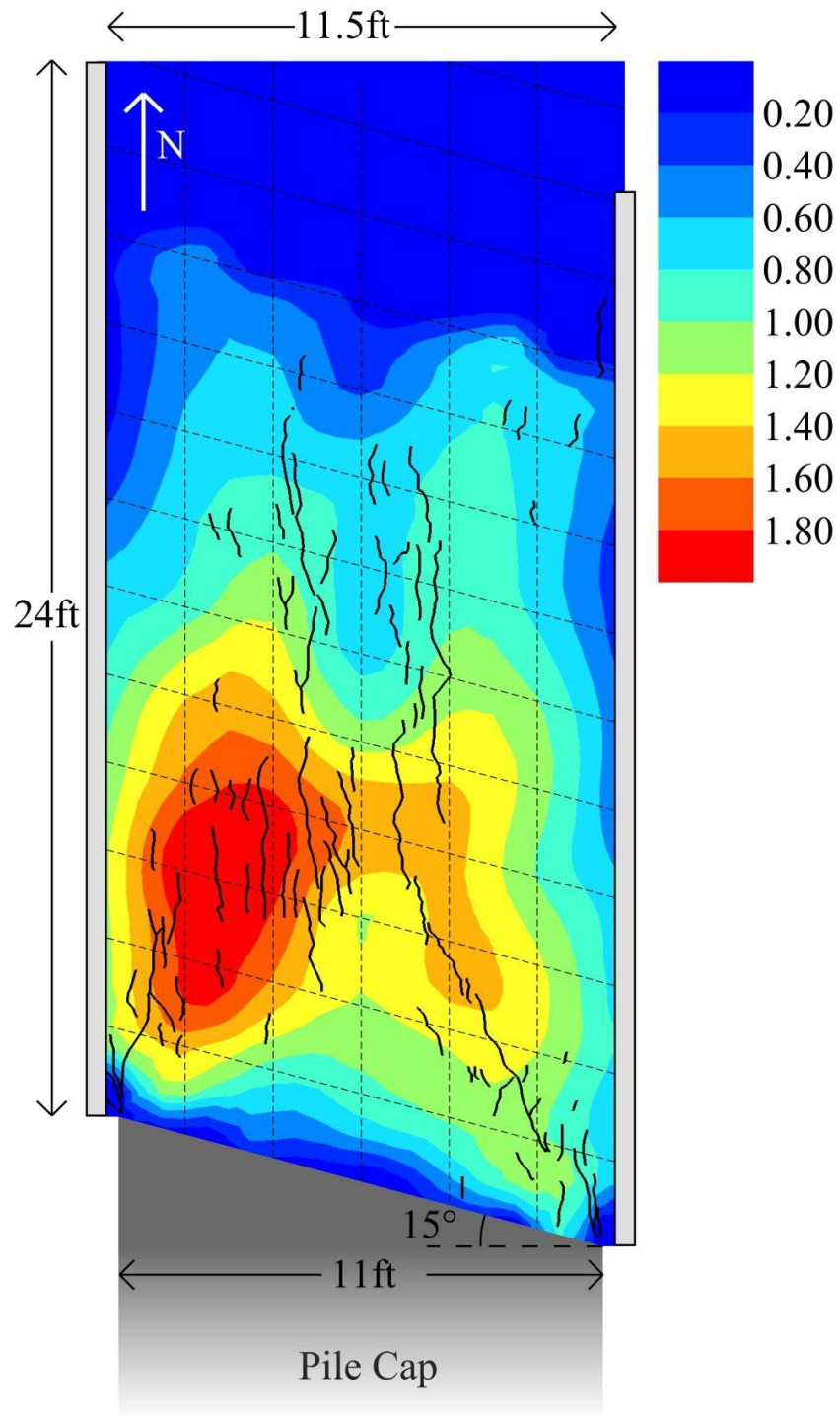
Figure 17. Vertical Backfill Displacement (Heave) in Inches for 15° Skew Test [Note: 1 in. = 25.4 mm and Gridlines are Spaced at 2-ft (0.61-m) Intervals].
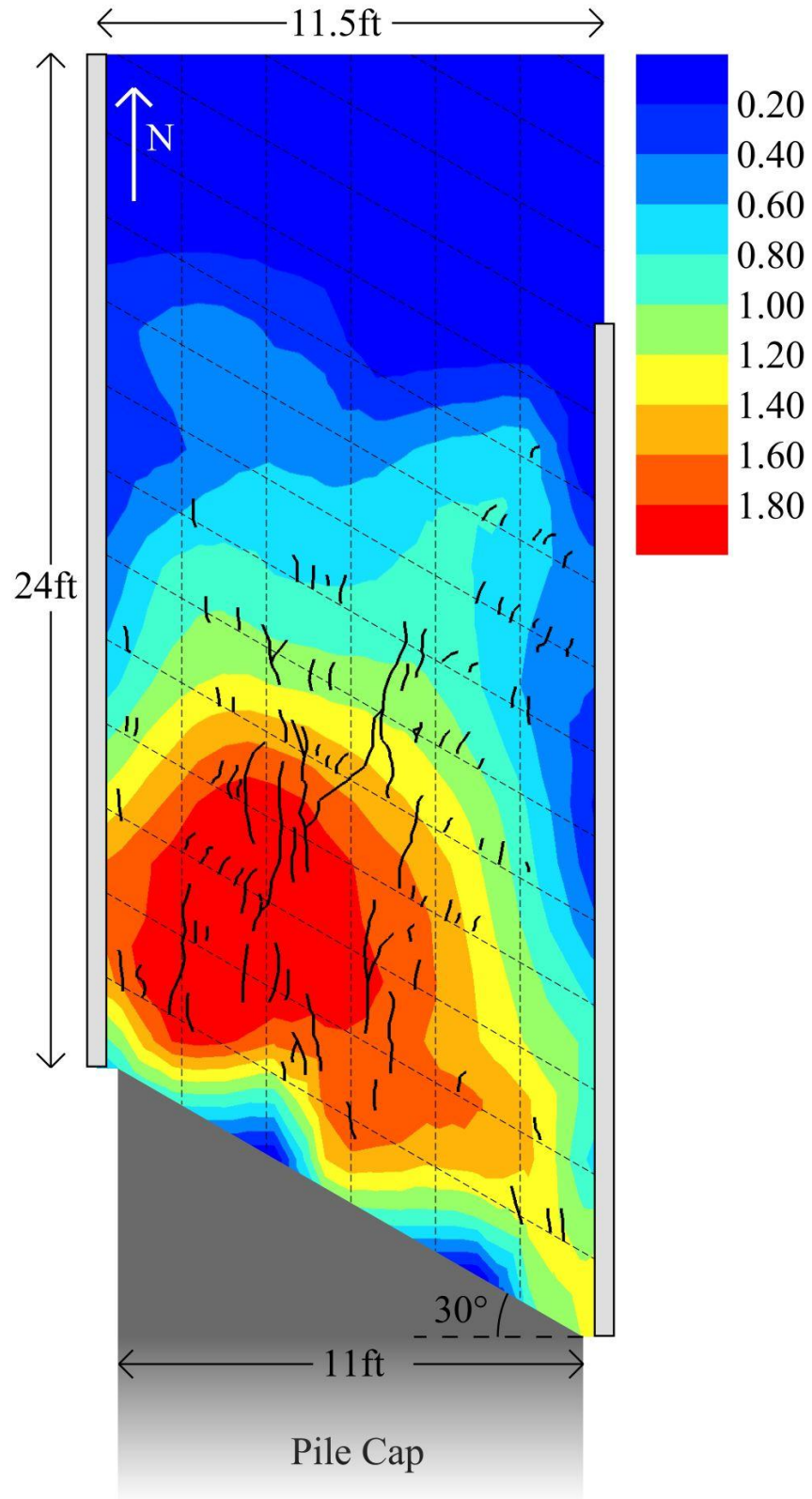
Figure 18. Vertical Backfill Displacement (Heave) in Inches for 30° Skew Test [Note: 1 in. = 25.4 mm and Gridlines are Spaced at 2-ft (0.61-m) Intervals].

For the 15° skew case, the horizontal displacement was measured using a total station and prism. Although limited in accuracy, these results provided a general estimate of direction and magnitude for horizontal displacement of the backfill surface. Figure 19 shows the displacement vector field (vector magnitude is increased factor of 3 for visualization) for the grid points painted onto the surface of the backfill. Additionally, Figure 20 shows this same displacement vector field; however, the four individual plots show displacements, δ, exceeding a minimum of 1.0, 2.0, 2.5 and 3.0 in (2.5, 5.1, 6.4 and 7.6 cm). The majority of the backfill experienced a minimum displacement of 1.0 in (2.54 cm), but 40% of the displacements greater than 3.0 in (7.6 cm) were located along the east wingwall.
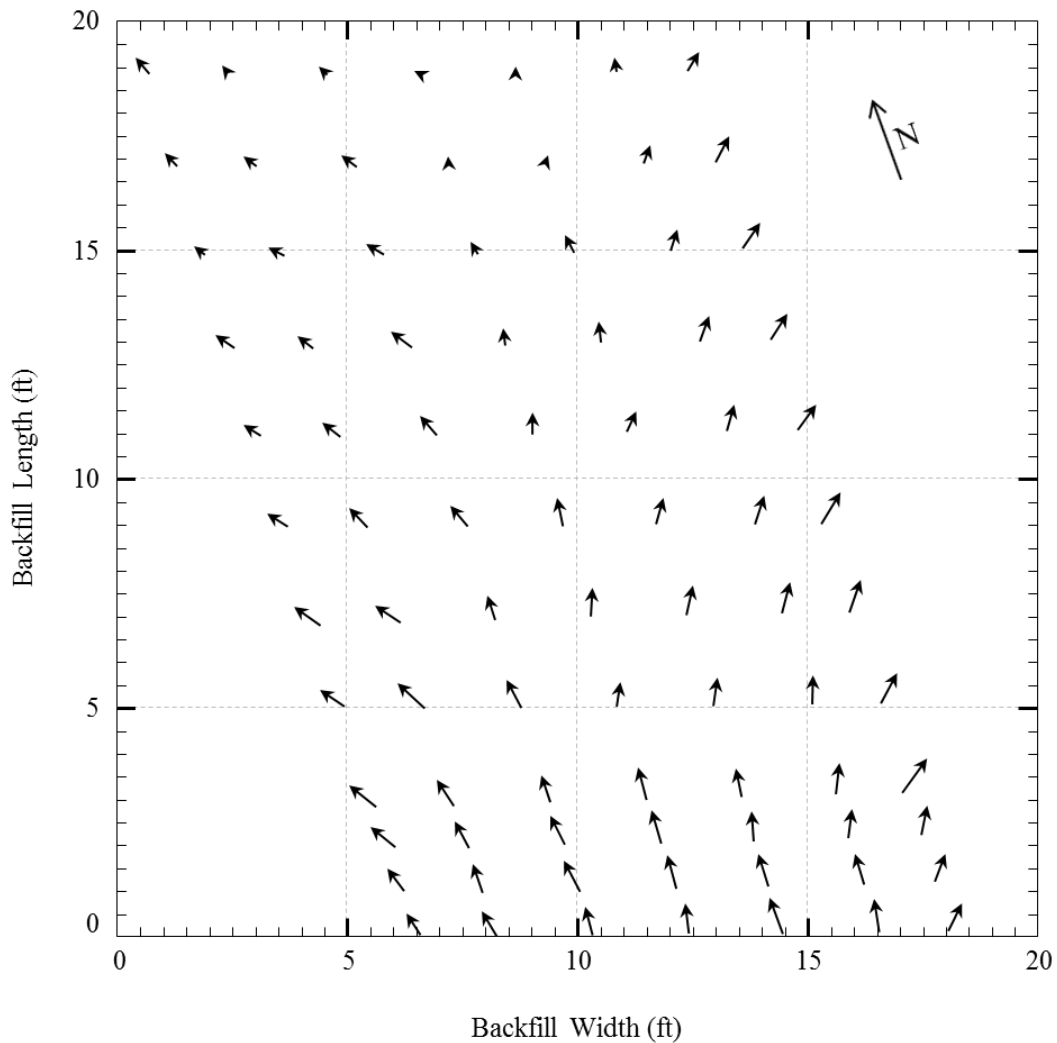
Figure 19. 15° Skew Backfill Displacement Vector Field (Displacement Scale: 3:1).

δ ≥ 1.0 in

δ ≥ 2.0 in

δ ≥ 2.5 in

δ ≥ 3.0 in
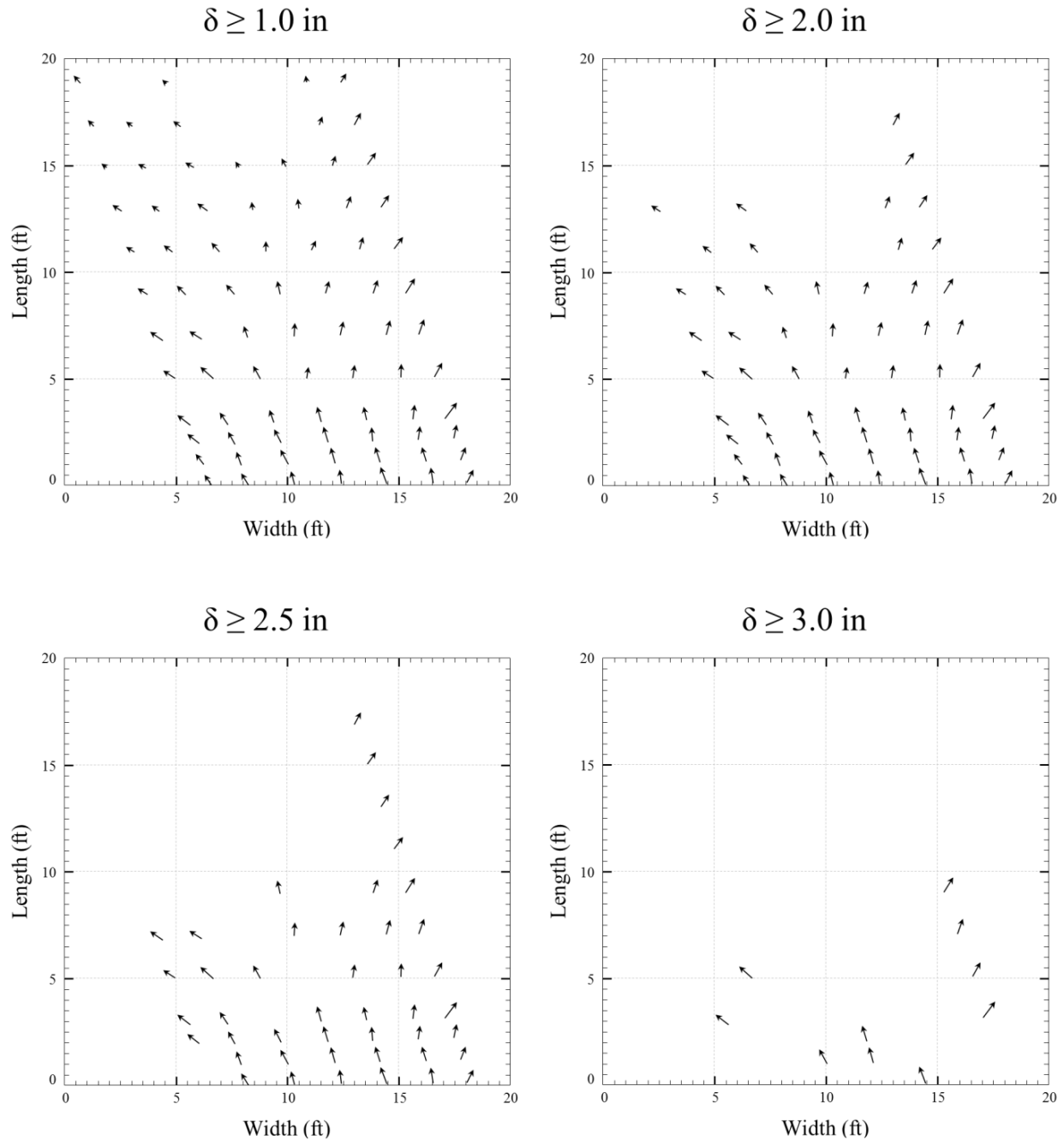
Figure 20. 15° Skew Backfill Displacement Vector Field with Specified Minimum Displacement (Displacement Scale: 3:1).

As the longitudinal displacement of the pile cap pushed into the soil, the soil moved both longitudinally and transverse causing the wingwalls to move outward. This led to an increase in the force in the MSE reinforcements which will be discussed subsequently in a more detailed report after the

strain gauge data has been reduced and analyzed.

CONCLUSIONS

1. Results of this large-scale field study confirm that there is a significant reduction in passive force as skew angles increase from 15° to 30° relative to non-skewed walls as observed in small-scale lab test results (Rollins and Jessee 2012) and numerical models (Shamsabadi et al. 2006) for densely compacted granular backfill.

2. The proposed passive-force reduction curve (Rollins and Jessee 2012) is confirmed and also validated for application with densely compacted granular backfill with MSE wingwalls.

3. For the 15° and 30° skew angles, the rate of strength gain decreased substantially at a pile-cap displacement of approximately 3% of the wall height. This decrease was much less pronounced for the 0° skew test.

4. Backwall pressure distribution is nonlinear. The largest pressures were located near the edges and lowest pressures were located near the center of the backwall face; however, the largest pressures developed on the acute side of the backwall. This is consistent with the larger vertical backfill displacement near the acute corner of the skew.

5. Additional large-scale tests, lab tests and/or numerical modeling should be completed with different abutment geometries (wall to height ratios), different soil types, and larger skew angles.

ACKNOWLEDGEMENTS

REFERENCES

AASHTO (2011). *Guide Specifications for LRFD Seismic Bridge Design*.

Apirakvorapinit, P., Mohammadi, J., and Shen, J. (2012). "Analytical Investigation of Potential Seismic Damage to a Skewed Bridge." *Practice Periodical on Structural Design and Construction*, 17(1), 5-12.

Burke, M. P., Jr. (1994). "Semi-Integral Bridges: Movements and Forces." *Transportation Research Record: Journal of the Transportation Research Board*, 1460, 1-7.

Caltrans, C. D. o. T. (2010). "Seismic Design Criteria, Version 1.6, November 2010." Division of Engineering Services, Office of Structure Design, Sacramento, California.

Christensen, D. S. (2006). "Full Scale Static Lateral Load Test of a 9 Pile Group in Sand." Master of Science, Brigham Young University, Provo, Utah.

Cole, R., and Rollins, K. (2006). "Passive Earth Pressure Mobilization during Cyclic Loading." *Journal of Geotechnical and Geoenvironmental Engineering*, 132(9), 1154-1164.

Duncan, J., and Mokwa, R. (2001). "Passive Earth Pressures: Theories and Tests." *Journal of Geotechnical and Geoenvironmental Engineering*, 127(3), 248-257.

Elias, V., and Christopher, B. R. (1997). "Mechanically Stabilized Earth Walls and Reinforced Soil Slopes, Design and Construction Guidelines." Federal Highway Administration.

Elnashai, A. S., Gencturk, B., Kwon, O.-S., Al-Qadi, I. L., Hashash, Y., Roesler, J. R., Kim, S. J., Jeong, S.-H., Dukes, J., and Valdivia, A. (2010). "The Maule (Chile) Earthquake of February 27, 2010: Consequence Assessment and Case Studies."

Kulhawy, F. and Mayne, P (1990). "Manual on Estimation of Soil Properties for Foundation Design, Report", *EPRI*-EL-6800. *Electric Power Research Institute*, Palo Alto, California**.**

Lee, K. L., and Singh, A. (1971). "Relative Density and Relative Compaction." *Journal of Soil Mechanics and Foundations Design*, 97(7), 1049-1052.

Lemnitzer, A., Ahlberg, E., Nigbor, R., Shamsabadi, A., Wallace, J., and Stewart, J. (2009). "Lateral Performance of Full-Scale Bridge Abutment Wall with Granular Backfill." *Journal of Geotechnical and Geoenvironmental Engineering*, 135(4), 506-514.

Rollins, K., and Sparks, A. (2002). "Lateral Resistance of Full-Scale Pile Cap with Gravel Backfill." *Journal of Geotechnical and Geoenvironmental Engineering*, 128(9), 711-723.

Rollins, K. M., Gerber, T. M., and Heiner, L. (2010). "Passive Force-Deflection Behavior for Abutments With MSE Confined Approach Fills." Brigham Young University Department of Civil & Environmental Engineering, Salt Lake City, UT, 83.

Rollins, K., Herbst, M., Gerber, T. and Cummins, C. (2009). "Monitoring Displacement vs. Depth in Lateral Pile Load Tests Using Shape Accelerometer Arrays." Procs. 17th Intl. Conf. on Soil Mech. and Geotech. Engrg. ISSMGE, IOS Press, Vol. 3, p. 2016-2019.

Rollins, K. M., and Jessee, S. J. (2012). "Passive Force-Deflection Curves for Skewed Abutments." *Journal of Bridge Engineering*, 17(5).

Sandford, T. C., and Elgaaly, M. (1993). "Skew Effects on Backfill Pressures at Frame Bridge Abutments." *Transportation Research Record: Journal of the Transportation Research Board*, 1-11.

Shamsabadi, A., Kapuskar, M., and Zand, A. (2006). "Three-Dimensional Nonlinear Finite-Element Soil-Abutment Structure Interaction Model for Skewed Bridges." *Fifth National Seismic Conference on Bridges & Highways*San Francisco, CA, 14.

Shamsabadi, A., Rollins, K. M., and Kapuskar, M. (2007). "Nonlinear Soil-Abutment-Bridge Structure Interaction for Seismic Performance-Based Design." *Journal of Geotechnical & Geoenvironmental Engineering*, 133(6), 14p.

Strassburg, A. N. (2010). "Influence of Relative Compaction on Passive Resistance of Abutments with Mechanically Stabilized Earth (MSE) Wingwalls." Master of Science, Brigham Young University, Provo, Utah.

Unjoh, S. "Repair and Retrofit of Bridges Damaged by the 2010 Chile, Maule Earthquake." *Proc., International Symposium on Engineering Lessons Learned from the 2011 Great East Japan Earthquake*.